JOURNAL OF GUIDANCE, CONTROL, AND DYNAMICS
Vol. 33, No. 5, September–October 2010

Control of the Electrodynamic Boom Propulsion System Accounting for Atmospheric Drag

Brian Wong* and Chris Damaren†
University of Toronto, Toronto, Ontario M3H 5T6 Canada

DOI: 10.2514/1.48972

Propulsion systems using the Lorentz force have previously been proposed to maneuver tethered spacecraft. The electrodynamic boom propulsion system extends the basic concept of electrodynamic tethers and replaces the conductive cable with more rigid appendages. This sidesteps some of the problems of using long tethers in space and could lift some of the restrictions in possible thrust directions at high orbit inclinations. This work examines an open-loop control algorithm to maneuver a spacecraft experiencing atmospheric drag using the thrust generated by three mutually orthogonal booms. The control algorithm is tested in simulation for several mission scenarios.

I. Introduction

ELECTRODYNAMIC propulsion is a concept that uses the force arising from the interaction between an electrical current in a conductive structure and a magnetic field to maneuver a satellite using little or no propellant. The direction of the force is related to the orientation of the conductive segment with respect to the local magnetic field lines and this could impose some limitation on possible thrust directions. Electrodynamic tethers are normally aligned close to the local vertical direction due to the gravity-gradient force, and they can only provide thrust in the along-track and cross-track directions. The flexible-body dynamics of tethers can also be complex and could have adverse consequences if left uncontrolled. A multiboom electrodynamic propulsion system operates in a similar manner as an electrodynamic tether, but the conductive segments are embedded inside several relatively short and rigid appendages. An orthogonal set of booms can provide thrust in almost any direction, and the structural dynamics of the booms are less complex than those of tethers.

Previous works on electrodynamic tethers could lend some valuable insight, since electrodynamic booms are similar to their tether counterparts in many ways. Boosting the orbit of a spacecraft using electrodynamic tethers is considered by Johnson and Herrmann [1] and Vas et al. [2], while autonomous deorbiting of a spacecraft was considered by Hoyt and Forward [3]. Carroll [4] developed a set of relations between current modulations and their effects on the orbital elements. Tragesser and San [5] developed a guidance scheme to perform general orbital maneuvers by applying the method of averaging to Gauss's form of the variational equations. Their solution is computationally simple but is not optimal, as the currents modulations and magnitudes are calculated at the beginning of the maneuver and are unchanged through the flight. Williams [6] demonstrated a method to optimally boost or deboost an orbit using the Gauss form of the variational equations as dynamic constraints and solving the problem using direct transcription. Tether librations are also explicitly considered in the optimal solution. Stevens and Wiesel [7] studied the optimal control of electrodynamic tethers over large time scales. They applied the method of averaging to a modified set of the variational equations and used the resulting linear equations as dynamic constraints for the optimal control problem, resulting in optimal currents that vary with time. Atmospheric drag is also included in their work. The dynamics and control of electrodynamic booms are comparatively less studied. Voronka et al. [8] examined the feasibility and the performance of an integrated propulsion and structural system in a Phase I study for NASA's Institute for Advanced Concepts. Their work looked at the state of the technologies relevant to the proposed system, especially in the areas of electron collection and emission, low mass structures, and electrical energy storage. They concluded that such systems are feasible and can provide performance comparable to other electric propulsion systems, but engineering challenges remain. Matthew and Voronka [9] developed two guidance algorithms for orbital maneuvering: a time-optimal open-loop law and a nonlinear Lyapunov feedback controller.

In this work, a two-part guidance scheme is developed to maneuver a satellite in the presence of atmospheric drag using a set of three mutually orthogonal booms. The work performed by Tragesser and San [5] for a single electrodynamic tether is extended for use with a multiboom system, and a drag compensation scheme is separately developed. The two schemes are then superimposed to give the final open-loop guidance law. This guidance law is then implemented in a numerical simulation and several scenarios are tested.

II. Equations of Motion

A spacecraft propelled by electrodynamic booms can be modeled as an arbitrary body with several rigid appendages extending from the satellite (Fig. 1). The development of the open-loop guidance scheme and subsequent analysis of the system are performed using two reference frames. The first is an inertial frame fixed at the center of the planet, with the $\mathbf{e_X}$ axis pointing toward Ares, the $\mathbf{e_Z}$ axis aligned with the rotation axis of the body, and $\mathbf{e_Y}$ completing the triad. The second frame is a spacecraft-centered orbital frame with $\mathbf{e_r}$ pointing from the center of the planet toward the spacecraft, $\mathbf{e_w}$ normal to the orbital plane, and $\mathbf{e_s}$ completing the triad in the along-track direction. To simplify the analysis, a classical set of orbital elements $[a \quad e \quad i \quad \Omega \quad \omega]$ is used to describe the spacecraft's position (provided the orbit eccentricity is nonzero), where a is the semimajor axis, e is the orbit eccentricity, is the orbit inclination, Ω is the right ascension of the ascending node, and ω is the argument of the periapsis. The orientation of the orbital frame relative to the inertial frame can be described using the orbital elements such that

$$\begin{bmatrix} \mathbf{e_r} \\ \mathbf{e_s} \\ \mathbf{e_w} \end{bmatrix} = C_3(\omega + v)C_1(i)C_3(\Omega) \begin{bmatrix} \mathbf{e_x} \\ \mathbf{e_y} \\ \mathbf{e_z} \end{bmatrix} \tag{1}$$

where $\mathbf{C}_i(\theta)$ is a rotation matrix about the ith axis and v is the true anomaly.

Received 18 January 2010; revision received 26 March 2010; accepted for publication 27 March 2010.

*NSERC Postdoctoral Fellow, Spacecraft Dynamics and Control Laboratory, Institute for Aerospace Studies, 4925 Dufferin Street.

†Associate Professor, Institute for Aerospace Studies, 4925 Dufferin Street. Associate Fellow AIAA.

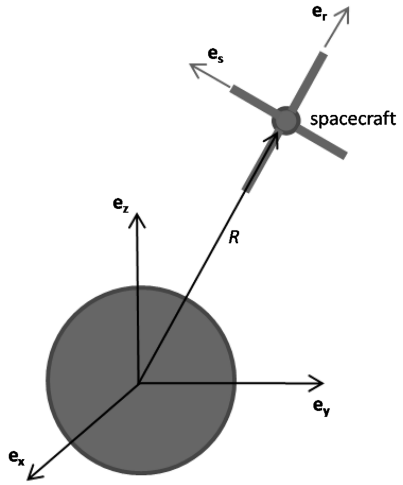

Fig. 1 Spacecraft model.

As the spacecraft orbits a planet with a magnetic field, currents flowing through the booms interact with the magnetic field such that the total Lorentz force acting on the system is given by

$$\mathbf{F} = \sum_{j=1}^{n} L_j I_j \mathbf{e}_j \times \mathbf{B} \tag{2}$$

where $\mathbf{e_j}$ is a vector tangential to the jth boom, L_j is the boom length, I_j is the total current flowing through that segment in the $\mathbf{e}_j$ direction, and $\mathbf{B}$ is the magnetic field of a planet. It can be seen in Eq. (2) that booms of different lengths and carrying different currents can be mathematically combined as long as they are aligned in the same direction.

The magnetic field is idealized as a simple dipole fixed at the centered of the planet with the magnetic axis $\mathbf{e_m}$ aligned with $\mathbf{e_z}$, implying that the magnetic equator is coincident with the geographic equator. The magnetic field is given by

$$\mathbf{B} = -\frac{\mu_m}{R^3}[3(\mathbf{e_r} \cdot \mathbf{e_m})\mathbf{e_r} - \mathbf{e_m}] \tag{3}$$

where μ_m is the magnetic moment of the dipole and R is the radial distance from the center of the planet to the spacecraft. This work considers an orthogonal set of three booms that are assumed to be permanently aligned with the $\mathbf{e_r}$, $\mathbf{e_s}$, and $\mathbf{e_w}$ direction. This is not a requirement for a realistic multiboom propulsion system and there could be some advantages in using a nonaligned setup. Using Eqs. (2) and (3) and working with $\mathbf{B}$ in the orbital frame, the total acceleration experienced by the spacecraft due to the electrodynamic forces are given by

$$\begin{aligned}\mathbf{a}_{\text{ele}} = \frac{\mu_m}{m_{\text{sat}}R^3}\{&[I_w L_w \cos(\omega+v)\sin(i) - I_s L_s \cos(i)]\mathbf{e_r} \\ &+ [2I_w L_w \sin(\omega+v)\sin(i) + I_r L_r \cos(i)]\mathbf{e_s} \\ &- [2I_s L_s \sin(\omega+v)\sin(i) + I_r L_r \cos(\omega+v)\sin(i)]\mathbf{e_w}\}\end{aligned} \tag{4}$$

where I_r, I_s, and I_w are currents flowing in the $\mathbf{e_r}$, $\mathbf{e_s}$, and $\mathbf{e_w}$ directions, respectively. Equation (4) also describes the acceleration imparted by an ideal gravity-gradient stabilized electrodynamic tether if I_s and I_w are set to zero. In a general orbit the electrodynamic tether can only generate thrust in the along-track and cross-track directions, while the orthogonal set of booms can thrust in all three directions even if a particular boom becomes parallel with the magnetic field line. A special case exists for equatorial orbits as neither the tethers nor the booms can push in the cross-track direction. Equation (4) also shows that it is inefficient to use the I_w current in low inclination orbits due to the $\sin(i)$ term, and this suggests that the cross-track current should be switched off for satellites operating in these orbits.

Electrodynamic tethers are more efficient than booms in converting currents into propulsive forces. Previous work by Estes et al. [10] have suggested that a 10 km tether can produce thrust in the order of 1 N using 10 A. An electrodynamic boom can only generate comparable forces by using very large currents as structural and spacecraft mass considerations limit its maximum length. This means the electrodynamic booms are better suited for orbit maintenance and small transfers than for large orbit changes. This problem cannot be circumvented by using additional segments if the total current is divided among the segments, such that the thrust generated by two 5-m-long booms, each carrying 2.5 A, is less than that generated by a 5 A current flowing down a 10 m segment. Multiple conductive booms may help in the collection of electrons from the ionosphere, however. The magnitude of $\mathbf{a}_{\text{ele}}$ at any time point also depends upon the instantaneous radius of the orbit, and the strength of the magnitude field drops off rapidly at higher orbits. The electrodynamic force can also be much weaker at apoapsis than at periapsis for highly elliptical orbits.

A. Open-Loop Current Law

The orbital maneuver portion of the guidance scheme seeks the appropriate current magnitudes and modulations to change the orbital elements of the spacecraft from some initial values $\mathbf{q}_0 = [\,a_0 \quad e_0 \quad i_0 \quad \Omega_0 \quad \omega_0\,]^T$ to final values $\mathbf{q}_f = [\,a_f \quad e_f \quad i_f \quad \Omega_f \quad \omega_f\,]^T$ within an allocated time span T. This scheme is developed from the Gauss form of the variational equation, given by Chobotov [11], using a method similar to Tragesser and San [5]. If the initial and final orbits have sufficiently low inclination and eccentricity such that $i \ll 1$ and $e \ll 1$, and assuming that no other external forces are acting on the spacecraft, then I_w can be dropped from Eq. (4) and the rates of change of the orbital elements due to $\mathbf{a}_{\text{ele}}$ are given by

$$\frac{\mathrm{d}a}{\mathrm{d}t} = \frac{\mu_m \cos(i)}{m_{\text{sat}}R^3}\left\{-\frac{2e\sin(v)I_s L_s}{n} + \frac{2aI_r L_r}{nR}\right\} \tag{5}$$

$$\frac{\mathrm{d}e}{\mathrm{d}t} = \frac{\mu_m \cos(i)}{m_{\text{sat}}R^3}\left\{-\frac{\sin(v)I_s L_s}{na} + \frac{(a^2-R^2)I_r L_r}{na^2 eR^2}\right\} \tag{6}$$

$$\frac{\mathrm{d}i}{\mathrm{d}t} = \frac{\mu_m \cos(\omega+v)\sin(i)}{m_{\text{sat}}R^2 na^2}\{I_r L_r \cos(\omega+v) + 2I_s L_s \sin(\omega+v)\} \tag{7}$$

$$\frac{\mathrm{d}\Omega}{\mathrm{d}t} = \frac{\mu_m \sin(\omega+v)}{m_{\text{sat}}R^2 na^2}\{I_r L_r \cos(\omega+v) + 2I_s L_s \sin(\omega+v)\} \tag{8}$$

$$\begin{aligned}\frac{\mathrm{d}\omega}{\mathrm{d}t} = \frac{\mu_m}{m_{\text{sat}}R^3}\Bigg\{&\frac{a\sin(v)}{e(\mu a)^{1/2}}\left(1+\frac{1}{1+e\cos(v)}\right)I_r L_r \cos(i) \\ &- \frac{\cos(v)I_s L_s \cos(i)}{nae} + \frac{\sin(\omega+v)\cos(i)}{a}(I_r L_r \cos(\omega+v) \\ &+ 2I_s L_s \sin(\omega+v))\Bigg\}\end{aligned} \tag{9}$$

where μ is the gravitational parameter of the planet. Previous works by Carroll [4] and Tragesser and San [5] have shown that secular changes in the orbital elements can be induced if I_r contains the terms $\cos(v)$, $\sin(v)$, $\cos(2\omega+2v)$, and $\sin(2\omega+2v)$ and a constant. The orbital elements can also be changed if I_s also contains those same terms, but each term would produce a different effect. For example, $I_r = 1$ and $I_s = \sin(v)$ will both produce secular changes in the semimajor axis with some coupling to other elements, while $I_r = \sin(v)$ and $I_s = 1$ will both produce secular changes in the argument of the periapsis ω. The currents in the radial and the transverse

directions used for orbital maneuvers are designated as i_r and i_s in order to distinguish them from the currents used for drag compensation to be discussed in the next section. They are given by

$$\begin{bmatrix} i_r \\ i_s \end{bmatrix} = \begin{bmatrix} a_1 + a_2\cos(v) + a_3\cos(2\omega + 2v) + a_4\sin(2\omega + 2v) + a_5\sin(v) \\ b_1\sin(v) + b_2\cos(v) + b_3\sin(2\omega + 2v) + b_4\cos(2\omega + 2v) + b_5 \end{bmatrix} \tag{10}$$

where a_i and b_i are current coefficients to be calculated by the guidance scheme and each coefficient has units of amperes. The terms of Eq. (10) are arranged in order of their effects on the orbital element set $[a \quad e \quad i \quad \Omega \quad \omega]$. The coefficients are calculated before the maneuver and remain static throughout the flight. The variational equations (5–9) describe both periodic and secular changes to the orbital elements, and the secular changes can be extracted by out by substituting Eq. (10) into Eqs. (5–9), changing the independent variable from t to v using $\mathrm{d}t = R^2[\mu a(1-e^2)]^{-1/2}\,\mathrm{d}v$, and then performing an averaging integral over one orbit. The orbital elements a, e, i, Ω, ω in the variational equations can be assumed to be constant and taken out of the integral if their changes are assumed to be small. The resulting system of equations describes only the secular rate of change and is linear with respect to the current coefficients. Let a vector designated as $\mathbf{\Delta} = \mathbf{q}_f - \mathbf{q}_0$ represent the desired orbital element changes and let $\mathbf{X} = [a_1 \quad a_2 \quad a_3 \quad a_4 \quad a_5 \quad b_1 \quad b_2 \quad b_3 \quad b_4 \quad b_5]^T$ be a vector of the current coefficients, then the current inputs are related to the orbital maneuver by

$$\Delta = T\mathbf{A}\mathbf{X} \tag{11}$$

where $\mathbf{A}$ is a 5×10 constant matrix and $\mathbf{A}\mathbf{X}$ represents the secular rate of change of the orbital elements. The elements of $\mathbf{A}$ are given in the Appendix. The $\mathbf{A}$ matrix is composed of two 5×5 blocks, with the left-hand block related to i_r and the right-hand block related to i_s. The offdiagonal terms in each block indicate coupling between the orbital elements and the different terms in the respective current law. If i_w is included in Eqs. (5–9), then an additional 5×5 block related to i_w is attached on the right-hand side of $\mathbf{A}$, making it a 5×15 matrix. Because of the change in the independent variable, the time of maneuver T now has units of radians and signifies the true anomaly required for the maneuver. Equation (11) describes an underdetermined system with 10 unknown current coefficients and only five equations and thus has an infinite number of solutions. One of the solutions can be calculated using

$$\mathbf{X} = \frac{1}{T}\mathbf{A}^+\mathbf{\Delta} \tag{12}$$

where $\mathbf{A}^+$ is the pseudoinverse of $\mathbf{A}$, given by $\mathbf{A}^+ = \mathbf{A}(\mathbf{A}\mathbf{A}^T)^{-1}$. This solution essentially minimizes $\mathbf{X}$, and hence the current, subjected to the constraint $\Delta - T\mathbf{A}\mathbf{X} = 0$. It should be noted that this solution is not time optimal. As T is inversely related to $\mathbf{X}$, the maximum current for the maneuver could be beyond the capacity of the spacecraft if the time of flight is too short. Should this be the case, the planned maneuver could be broken up into several smaller maneuvers, such that the current draw satisfies the power system constraints.

The open-loop guidance scheme assumes that there are no other forces acting on the spacecraft besides the electrodynamic force. However, in low Earth orbits, the atmospheric drag has noticeable effects on the satellite orbit and should be accounted for. This is especially important for the electrodynamic satellite, as they require more time to perform any maneuver and hence experience drag for a greater amount of time.

B. Atmosphere Drag Compensation

Atmospheric drag decreases the orbital energy of a spacecraft and causes secular changes to its semimajor axis and eccentricity. Conventional satellites can perform periodic orbit maintenance to correct the drift, but the limited onboard fuel supply restricts the operational life of the spacecraft. As a propulsion system using electrodynamic forces consumes little to no fuel, the effects of atmospheric drag can be continuously compensated by applying properly modulated currents. One method of determining the required currents is to estimate the effect of drag on the orbital elements using the orbital perturbations equations, then using Eq. (12) to find the current coefficients to compensate for the expected changes. This method can be repeated at regular intervals. One weakness to this approach is that the atmospheric density is only updated when new current coefficients are calculated, and this implicitly assumes that the drag force holds constant between the updates. Satellites in elliptical orbits will experience a time-varying drag and this method causes the controller to under estimate the required currents. A second method is to estimate the drag force experienced by the spacecraft and to continuously apply compensating forces. Accurate descriptions of the drag forces require a detailed model of the atmosphere as well as an accurate estimate of the spacecraft states. Detailed aerodynamic analysis of the electrodynamic spacecraft is beyond the scope of this paper, but an estimate of the current magnitudes required for drag mitigation can be obtained using a first-order analysis.

An approximation of the drag acceleration encountered by a spacecraft expressed in the orbital frame is given by

$$\mathbf{a}_{\text{drag}} = \begin{bmatrix} -\frac{1}{2}\frac{\rho(h)C_dA}{m_{\text{sat}}}v_{\text{rel}}^2\sin(\gamma) \\ -\frac{1}{2}\frac{\rho(h)C_dA}{m_{\text{sat}}}v_{\text{rel}}^2\cos(\gamma) \\ 0 \end{bmatrix} \tag{13}$$

where $\rho(h)$ is the atmospheric density at altitude h, C_d is the drag coefficient, A is the spacecraft frontal area, m_{sat} is the spacecraft mass, v_{rel} is the spacecraft velocity relative to the atmosphere, and γ is the flight-path angle. If the atmosphere is assumed to be static, then v_{rel} is the spacecraft velocity and can be approximated by the equation

$$v_{\text{rel}} = \left[\frac{\mu(1 + 2e\cos(v) + e^2)}{a(1-e^2)}\right]^{1/2} \tag{14}$$

The flight-path angle γ can also be calculated from the orbital elements, and $\sin(\gamma)$ and $\cos(\gamma)$ are given by

$$\sin(\gamma) = \frac{e\sin(v)}{(1 + 2e\cos(v) + e^2)^{1/2}} \tag{15}$$

$$\cos(\gamma) = \frac{1 + e\cos(v)}{(1 + 2e\cos(v) + e^2)^{1/2}} \tag{16}$$

While the e^2 terms are omitted in the development of the orbital maneuver scheme, they are retained here to improve the accuracy of the drag estimation and to add flexibility to the drag compensation scheme. In this analysis, the atmospheric density is modeled using a simple exponential law given by

$$\rho = \rho_0 e^{\frac{[h - h_{\text{ref}}]}{H}} \tag{17}$$

where ρ_0 is the reference density used with the reference altitude h_{ref}, h is the altitude of the spacecraft, and H is the scale height. The values for ρ_0, h_{ref}, and H can be found in texts such as Vallado [12]. More refined atmospheric models can be used for more detailed studies of the system. Substituting Eqs. (14–17) into Eq. (13) and dropping i_w, the current required to compensate the drag deceleration can be calculated using $\mathbf{a}_{\text{ele}} - \mathbf{a}_{\text{drag}} = \mathbf{0}$:

$$i_{r_{\text{drag}}} = \frac{\rho C_dA\mu a^2(1-e^2)^2 e\sin(v)(1 + 2e\cos(v) + e^2)^{1/2}}{2\mu_m L_r(1 + e\cos(v))^3\cos(i)} \tag{18}$$

$$i_{s_{\text{drag}}} = \frac{\rho C_dA\mu a^2(1-e^2)^2(1 + 2e\cos(v) + e^2)^{1/2}}{2\mu_m(1 + e\cos(v))^2 L_s\cos(i)} \tag{19}$$

The electrodynamic force required to counteract drag can be found using Eq. (2). The product C_dA could be estimated during the initial checkout period, and the true anomaly v could be linked to the mission clock via Kepler's equation. Equations (18) and (19) should be updated periodically with new estimates of the atmospheric density and orbital elements and if the spacecraft is maneuvered. The drag compensation currents $i_{r_{\text{drag}}}$ and $i_{s_{\text{drag}}}$ can be superimposed on top of the orbital maneuver currents such that the total current flowing through the electrodynamic segments are given by

$$\begin{bmatrix} I_r \\ I_s \end{bmatrix} = \begin{bmatrix} i_r + i_{r_{\text{drag}}} \\ i_s + i_{s_{\text{drag}}} \end{bmatrix} \tag{20}$$

III. Numerical Results

Numerical simulations are used to access the performance of the electrodynamic propulsion system for several orbit maneuvers. The equation of motion for the spacecraft is given by

$$\ddot{\mathbf{R}} = -\frac{\mu}{R^3}\mathbf{R} + \mathbf{a}_{\text{ele}} + \mathbf{a}_{\text{drag}} \tag{21}$$

where $\mathbf{R}$ is the position vector of the spacecraft in the inertial frame, μ is the gravitational parameter, $\mathbf{a}_{\text{ele}}$ is the acceleration due to the Lorentz forces, and $\mathbf{a}_{\text{drag}}$ is the drag acceleration. In all the simulations, the Earth-orbiting spacecraft has a mass of 200 kg, L_r and L_s are both 30 m long, and the frontal area A is 2 m^2. For drag modeling, the reference altitude h_{ref} chosen is 300 km, the scale height H is 53.628 km, and the reference density ρ_0 is 2.418×10^{-11} kg/m^3.

A. Orbit Maintenance

This example demonstrates the ability of the electrodynamic spacecraft to maintain its orbit in the presence of drag. The spacecraft is initially in a near circular orbit, with orbital elements given by

$$[\,a_0 \quad e_0 \quad i_0 \quad \Omega_0 \quad \omega_0\,] = [\,6752\text{ km} \quad 0.005 \quad 10^\circ \quad 50^\circ \quad 30^\circ\,]$$

Figure 2 shows the change in the spacecraft's orbital elements over time for two scenarios, one including aerodynamic drag only and one with drag correction. It can be seen the satellite's semimajor axis decreased by 4.417 km over 150 h due to drag, and small changes also developed in the eccentricity. The drag correction forces are continuously applied, with the atmospheric density $\rho(h)$ constantly updated in the simulation. As such, this is the ideal case for drag correction. The applied electrodynamic forces are capable of negating the effects of drag on the semimajor axis and the eccentricity, but the inclination and the right ascension of the node are reduced at a constant rate, with the change in inclination the more dominant effect. The radial current $i_{r_{\text{drag}}}$ varies between 0.623 and 2.195 A, while along-track current $i_{s_{\text{drag}}}$ has a much smaller range between −0.006 and 0.007 A. Figure 3 shows the current usage over time and Fig. 4 is a close-up of Fig. 3 over 10 h.

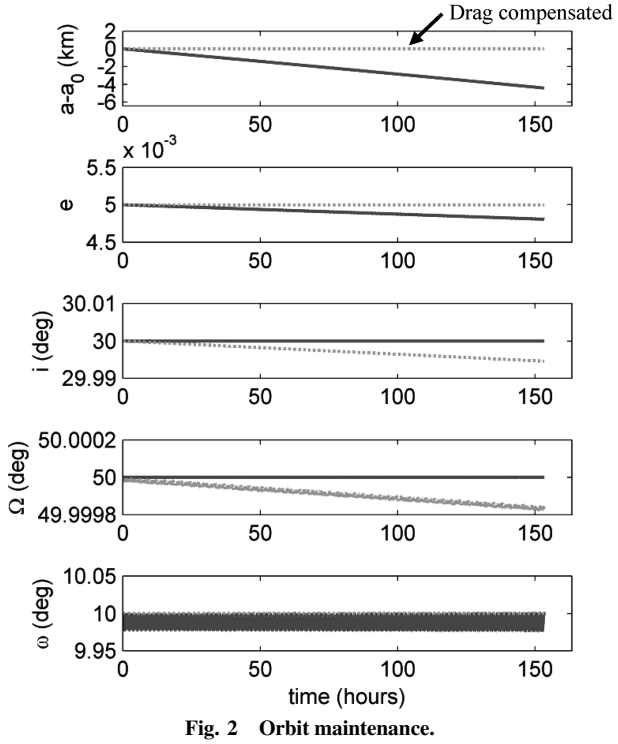

Fig. 2 Orbit maintenance.

B. Orbit Raising

This example looks at increasing the orbit semimajor axis by 10 km in 80 orbits, with $T = 502.655$ rad or 122 h, while keeping the other orbital elements constant. The initial elements of the spacecraft are given by

$$[\,a_0 \quad e_0 \quad i_0 \quad \Omega_0 \quad \omega_0\,] = [\,6752\text{ km} \quad 0.005 \quad 30^\circ \quad 50^\circ \quad 30^\circ\,]$$

and $\mathbf{\Delta}$ is given by $[\,10\text{ km} \quad 0 \quad 0 \quad 0 \quad 0\,]^T$. The required currents are calculated by Eq. (12) and they are given by

$$i_r = [3.816 - 0.003\cos(v) - 1.526\cos(2\omega + 2v) + 0.001\sin(v)]A \tag{22}$$

$$i_s = [0.001\sin(v) - 3.053\sin(2\omega + 2v)]A \tag{23}$$

The current i_r mostly serves to raise the orbit, while i_s serves to maintain inclination due to the coupling in the $\mathbf{A}$ matrix. The guidance scheme discontinues the orbital maneuver currents after time T, while the drag compensation currents are always active.

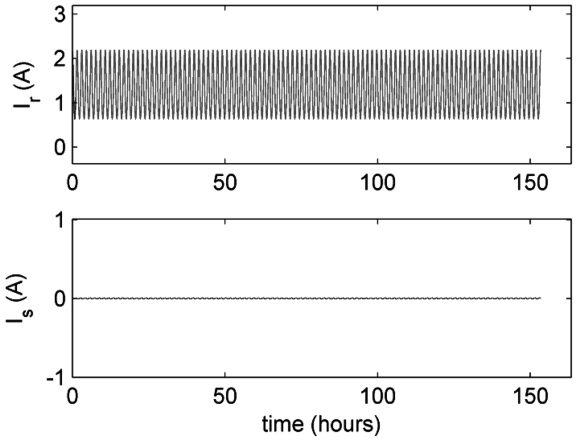

Fig. 3 Current used for drag correction.

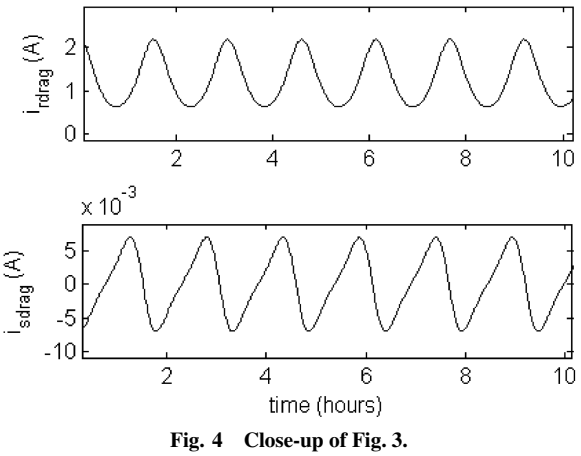

Fig. 4 Close-up of Fig. 3.

Figure 5 shows the maneuver with and without the drag compensation forces, and it can be seen that the spacecraft's semimajor axis only increased by 6.806 km instead of 10 km without drag compensation. The relatively long time of maneuver allows more orbital energy to be sapped by atmospheric drag. This error can be minimized using a faster transfer at the cost of higher maximum currents, as the spacecraft escapes the relatively thicker portion of the atmosphere in less time. The orbit is successfully raised when both orbital maneuver and drag compensation currents are used, but the inclination is affected by the application of $i_{r_{\text{drag}}}$ and $i_{s_{\text{drag}}}$. Figure 6 shows the total current draw, including both orbital maneuver and the drag compensation currents, over time. The maximum I_r is 6.712 A and this occurs at the start of the maneuver, gradually decreasing over time as the orbital radius increases and the spacecraft experiences less drag. The maximum I_s is 3.058 A and this does not change over time. The current requirements are greatly reduced after 122 h, after the orbital maneuver currents are switched off.

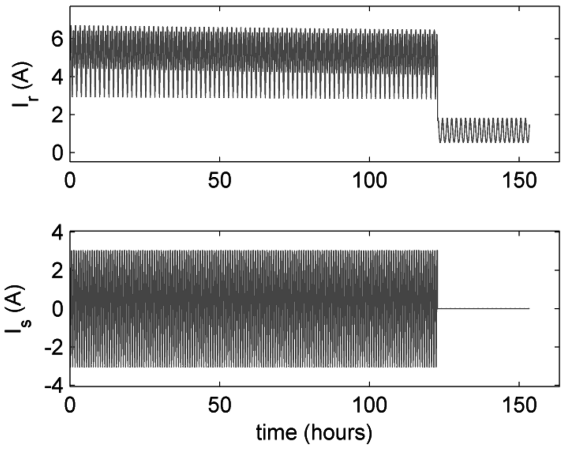

Fig. 6 Total current usage.

C. Inclination Change and Combined Maneuver

The final two examples examine a maneuver with an orbit inclination change only and with a combined maneuver incorporating a semimajor axis change with an inclination change. The initial orbital elements are again given by

$$[\,a_0 \quad e_0 \quad i_0 \quad \Omega_0 \quad \omega_0\,] = [\,6752\ \text{km} \quad 0.005 \quad 30^\circ \quad 50^\circ \quad 30^\circ\,]$$

The first maneuver is to decrease the inclination by 0.5 deg while maintaining the other elements constant, such that $\Delta_i = [\,0 \quad 0 \quad -0.5^\circ \quad 0 \quad 0\,]^T$. The time of maneuver is 200 orbits, or $T = 1256$ rad. The current coefficients are calculated using Eq. (12) and i_r and i_s are given by

$$i_r = [0.047\cos(v) + 24.923\cos(2\omega + 2v) - 0.009\sin(v)]A \quad (24)$$

$$i_s = [-0.023\sin(v) - 0.004\cos(v) + 49.845\sin(2\omega + 2v)]A \quad (25)$$

The combined maneuver is expressed by $\Delta_c = [\,100\ \text{km} \quad 0 \quad -0.5^\circ \quad 0 \quad 0\,]^T$, and the required currents are given by

$$i_r = [15.263 + 0.035\cos(v) + 18.818\cos(2\omega + 2v) - 0.006\sin(v)]A \quad (26)$$

$$i_s = [-0.018\sin(v) - 0.003\cos(v) + 32.635\sin(2\omega + 2v)]A \quad (27)$$

Comparing Eqs. (24–27), it can be seen that the combined maneuver is a little less costly than just the inclination change alone. As applying a constant current to increase the semimajor axis has the effect of decreasing the orbit inclination, this maneuver takes advantage of the coupling to lower the cost of maneuver. Cost savings can also be obtained by simultaneously lowering the semimajor axis and increasing the inclination, but this increases the drag on the spacecraft. Raising the orbit also reduces the drag encountered by the satellite and lowers the drag mitigation currents. The previous two examples also show that the drag compensation forces also decrease the inclination, but the guidance is entirely separate from the drag compensation scheme and cannot take advantage of this effect. Figure 7 shows that the results of the inclination change and drag are not factors in the accuracy of the maneuver. The cost of the maneuver is shown in Fig. 8, and the maximum current draw is 77.009 A. Figure 9 shows the results of the

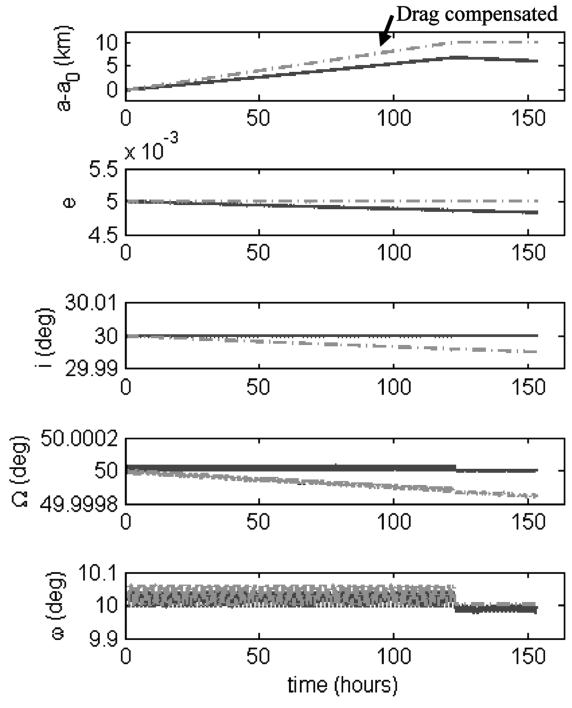

Fig. 5 A 10 km orbit rising.

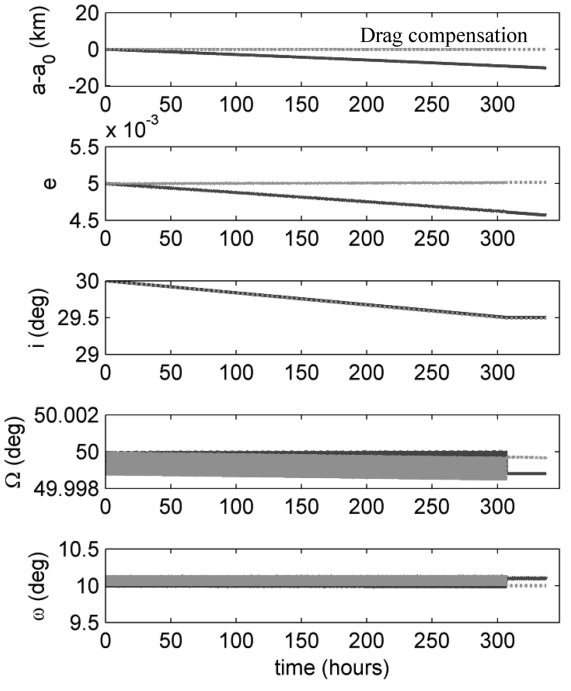

Fig. 7 Inclination change only.

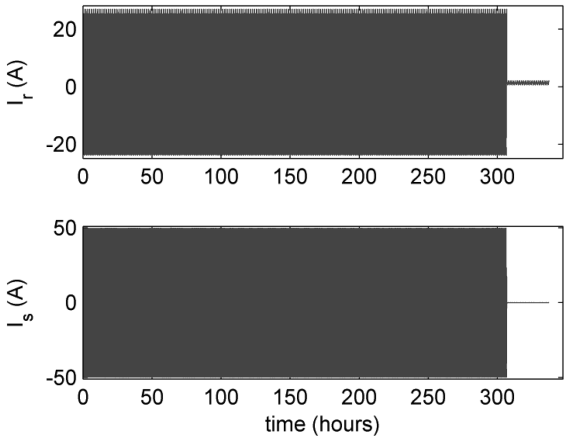

Fig. 8 Current required for inclination change.

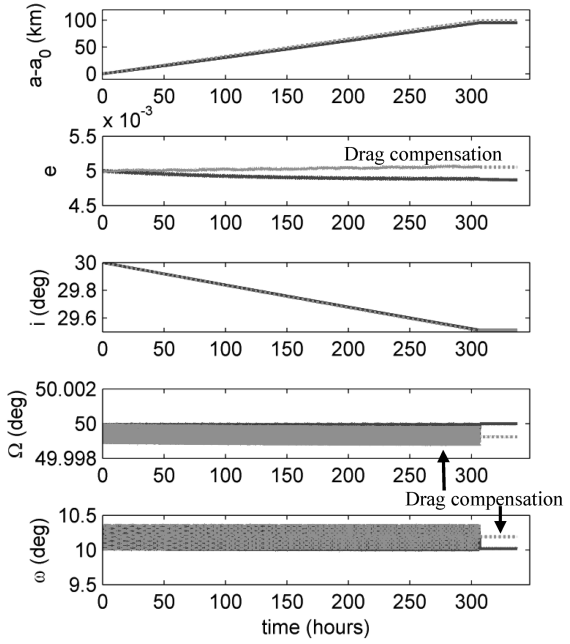

Fig. 9 Combined orbital element change.

combined maneuver and verifies that making larger semimajor axis changes over a short amount of time increases the accuracy of the maneuver, as the difference between with drag correction and without drag correction is only 3.974 km. The maximum current draw is 73.888 A, and a time history of the current usage is shown in Fig. 10. The electrodynamic booms most likely will not be able to collect sufficient amounts of electron from the Earth's ionosphere to supply the current required for the two above scenarios. The conductive elements in the booms will also have some electrical resistance, and there is a risk that high currents will generate enough heat to damage the system. Tragesser and San [5] suggested a method to phase the orbital maneuver such that the current draw stays below a defined limit, and their method could be applied here to lower the maximum current draw at the expense of increased maneuver time.

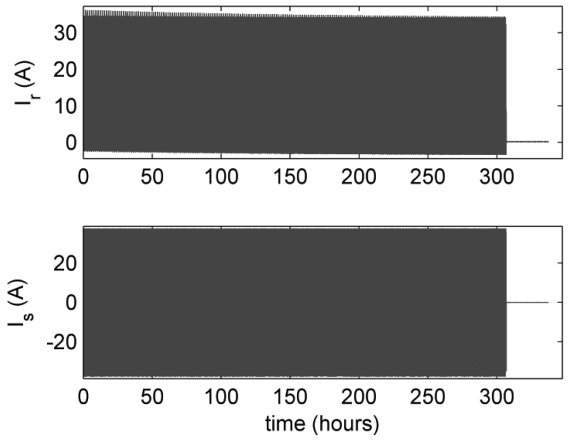

Fig. 10 Current draw.

IV. Conclusions

The analysis showed that the multiboom electrodynamic propulsion system is capable of making small changes to a spacecraft's orbit, and the propellantless nature of this system makes it suitable for long-duration spacecraft. The open-loop control scheme developed in this work is not computationally intensive. The effects of atmospheric drag on the electrodynamic spacecraft should be taken into account, given the time required for this system to perform orbital maneuvers. Future works include extending the guidance scheme to integrate drag compensation with orbital maneuver and examining the effects of structural flexibility on the performance of the electrodynamic system.

Appendix: Matrix A Entries

The entries of the **A** matrix are given below. The constant Φ is defined as $\Phi = \mu_m / m_{\text{sat}}\mu$, where μ_m is magnetic dipole of the magnetic field, m_{sat} is the total mass of the satellite, and μ is the gravitational constant of the planet:

$$A_{1,1} = 2\Phi L_r \cos i_0 \qquad A_{1,2} = 2\Phi e_0 L_r \cos i_0 \qquad A_{1,3} = 0$$
$$A_{1,4} = 0 \qquad A_{1,5} = 0 \qquad A_{1,6} = -\Phi e_0 L_s \cos i_0 \qquad A_{1,7} = 0$$
$$A_{1,8} = 0 \qquad A_{1,9} = 0 \qquad A_{1,10} = 0$$

$$A_{2,1} = 0 \qquad A_{2,2} = \frac{\Phi L_i \cos i_0}{a_0} \qquad A_{2,3} = 0 \qquad A_{2,4} = 0$$
$$A_{2,5} = 0 \qquad A_{2,6} = -\frac{\Phi L_s \cos i_0}{2a_0} \qquad A_{2,7} = 0$$
$$A_{2,8} = -\frac{\Phi L_s e_0 \cos 2\omega_0 \cos i_0}{4a_0} \qquad A_{2,9} = \frac{\Phi L_s e_0 \sin 2\omega_0 \cos i_0}{4a_0}$$
$$A_{2,10} = 0$$

$$A_{3,1} = -\frac{\Phi L_r \sin i_0}{2a_0} \qquad A_{3,2} = 0 \qquad A_{3,3} = \frac{\Phi L_r \sin i_0}{4a_0}$$
$$A_{3,4} = 0 \qquad A_{3,5} = 0$$

$$A_{4,1} = 0 \qquad A_{4,2} = 0 \qquad A_{4,3} = 0 \qquad A_{4,4} = -\frac{\Phi L_r}{4a_0}$$
$$A_{4,5} = 0 \qquad A_{4,6} = 0 \qquad A_{4,7} = 0 \qquad A_{4,8} = 0$$
$$A_{4,9} = \frac{\Phi L_s}{2a_0} \qquad A_{4,10} = \frac{\Phi L_s}{a_0}$$

$$A_{5,1} = 0 \qquad A_{5,2} = 0 \qquad A_{5,3} = -\frac{\Phi L_r \sin 2\omega_0 \cos i_0}{4a_0}$$
$$A_{5,4} = \frac{\Phi L_r \cos^2 \omega_0 \cos i_0}{2a_0} \qquad A_{5,5} = \frac{\Phi L_r \cos i_0}{a_0 e_0} \qquad A_{5,6} = 0$$
$$A_{5,7} = \frac{\Phi L_s \cos i_0}{2a_0 e_0} \qquad A_{5,8} = \frac{\Phi L_s \sin 2\omega_0 \cos i_0}{4a_0}$$
$$A_{5,9} = \frac{\Phi L_s \cos i_0}{2a_0}\left(\cos^2 \omega_0 - \frac{3}{2}\right) \qquad A_{5,10} = \frac{3\Phi L_s \cos i_0}{2a_0}$$

Acknowledgment

This work is supported by the Natural Sciences and Engineering Research Council of Canada (NSERC) Postdoctoral Fellowship Award.

References

[1] Johnson, L., and Herrmann, M., "International Space Station Electrodynamic Tether Reboost Study," NASA TM-1998-208538, 1998.

[2] Vas, I. E., Kelly, T. J., and Scarl, E., "Application of an Electrodynamic Tether System to Reboost the International Space Station," *Proceedings of the Tether Technology Interchange Meeting*, NASA CP-1998-206900, 1998.

[3] Hoyt, R. P., and Forward, R. L., "Performance of the Terminator Tether for Autonomous Deorbit of LEO Spacecraft," 5th AIAA/ASME/SAE/ASEE Joint Propulsion Conference, Los Angeles, AIAA Paper 99-2839, June 1999.

[4] Carroll, J., *Guidebook for Analysis of Tether Applications*, Martin Marietta, Raleigh, NC, 1985.

[5] Tragesser, S., and San, H., "Orbital Maneuvering with Electrodynamic Tethers," *Journal of Guidance, Control, and Dynamics*, Vol. 26, No. 5, 2003, pp. 805–810. doi:10.2514/2.5115

[6] Williams, P., "Optimal Orbital Transfer with Electrodynamic Tether," *Journal of Guidance, Control, and Dynamics*, Vol. 28, No. 2, 2005, pp. 369–371. doi:10.2514/1.12016

[7] Stevens, R., and Wiesel, W., "Large Time Scale Optimal Control of an Electrodynamic Tether Satellite," *Journal of Guidance, Control, and Dynamics*, Vol. 31, No. 6, 2008, pp. 1716–1727. doi:10.2514/1.34897

[8] Voronka, N., Hoyt, R., Slostad, J., Gilchrist, B., and Fuhrhop, K., *Modular Spacecraft with Integrated Structural Electrodynamic Propulsion*, NASA Inst. for Advanced Concepts, Universities Space Research Association, Atlanta, 2006.

[9] Matthew, A., and Voronka, N., "Control of a Multi-Beam Electrodynamic Spacecraft Propulsion System," *2008 American Control Conference*, Seattle, WA, 2008.

[10] Estes, R. D., Lorenzini, E. C., Sanmartin, J., Pelaez, J., Martinez-Sanchez, M., Johnson, C. L., Vas, I. E., et al., "Bare Tethers for Electrodynamic Spacecraft Propulsion," *Journal of Spacecraft and Rockets*, Vol. 37, No. 2, March–April 2000, pp. 205–211. doi:10.2514/2.3567

[11] Chobotov, V. A., *Orbital Mechanics*, AIAA, Washington, D.C., 1991.

[12] Vallado, D., *Fundamentals of Astrodynamics and Applications*, Microcosm Press, El Segundo, CA, 2001.